

Triplex-Forming Oligonucleotides

A Click Chemistry Approach to Targeted DNA Crosslinking with *cis*-Platinum(II)-Modified Triplex-Forming Oligonucleotides

Joseph Hennessy, Bríonna McGorman, Zara Molphy, Nicholas P. Farrell, Daniel Singleton, Tom Brown, and Andrew Kellett*

Abstract: Limitations of clinical platinum(II) therapeutics include systemic toxicity and inherent resistance. Modern approaches, therefore, seek new ways to deliver active platinum(II) to discrete nucleic acid targets. In the field of antigene therapy, triplex-forming oligonucleotides (TFOs) have attracted interest for their ability to specifically recognise extended duplex DNA targets. Here, we report a click chemistry based approach that combines alkyne-modified TFOs with azide-bearing *cis*-platinum(II) complexes—based on cisplatin, oxaliplatin, and carboplatin motifs—to generate a library of Pt^{II}-TFO hybrids. These constructs can be assembled modularly and enable directed platinum(II) crosslinking to purine nucleobases on the target sequence under the guidance of the TFO. By covalently incorporating modifications of thiazole orange—a known DNA-intercalating fluorophore—into Pt^{II}-TFOs constructs, enhanced target binding and discrimination between target and off-target sequences was achieved.

Introduction

Therapies that target the downstream inhibition of gene expression are of great current research significance, with

considerable efforts now dedicated to the discovery of new antisense oligonucleotides (ASOs).^[1] The development of nucleic acid probes targeting DNA, such as triplex-forming oligonucleotides (TFOs),^[2] offers an alternative strategy, whereby gene expression is directly inhibited at the genomic level. Here, we present a click chemistry strategy for the generation of a new class of *cis*-platinum(II)-TFO hybrid biomaterials that possess DNA binding and crosslinking activity. Homopyrimidine TFOs (containing T and C bases only) bind non-covalently in the major groove of duplex DNA to purine-rich target strands through Hoogsteen hydrogen bond formation with AT and GC base pairs to produce T-AT and C⁺-GC parallel triplex motifs.^[3]

One of the main challenges confronting the application of TFOs is their weak duplex binding affinity and poor in vitro and in vivo stability.^[4] Recent work has, therefore, focused on enhancing target binding properties and maximising their lifetimes in cellular environments. As part of this effort, the introduction of a covalent crosslinking agent such as psoralen into TFO constructs has shown significant promise (Figure S-1).^[5] Here, crosslinking is initiated by UV light^[6] to produce gene-specific mutations^[7] that inhibit transcriptional activity.^[8] Alternatively, the use of TFOs as targeting probes that discretely transport platinum(II) crosslinking agents to selected duplex targets has also been explored.^[9] Several motifs exist but sustained efforts to coordinate *trans*-Pt^{II} complexes—such as *trans*-dichlorodiammineplatinum(II)—to a guanine (mismatch) base within TFO constructs has enabled the generation of mono-functional crosslinking hybrids (Figure S-1).^[10] Here, a single labile *trans* site on the probe-bound Pt^{II} complex is available to crosslink with a purine base on the target duplex. Although mono-functional Pt^{II}-TFOs have previously been generated through platinum-derivatised phosphoramidites^[11] and solid-phase synthesis of tethered *trans*-Pt^{II} motifs,^[12] surprisingly little research has been carried out to extend this concept towards the construction of bifunctional cisplatin(II)-TFO motifs. Further attempts to incorporate platinated nucleotide building blocks into oligonucleotides (ON) using solid-phase synthesis have yielded inactive platinum products,^[13] although a *cis*-platinum(II)-tethered ON was shown to retain crosslinking ability and displayed adduct formation against a 25:29-mer duplex target (Figure S-1).^[14]

From a design perspective, there are notable obstacles that restrict the potential of existing Pt-TFO hybrid motifs, including: 1) *trans*-Pt^{II}-TFOs are limited by their need to incorporate a mismatched guanine base to which the *trans*-platinum(II) reagent is coupled; 2) the geometry of *cis*-


[*] J. Hennessy, B. McGorman, Dr. Z. Molphy, Prof. A. Kellett
 School of Chemical Sciences and National Institute for Cellular
 Biotechnology, Dublin City University
 Glasnevin, Dublin 9 (Ireland)
 E-mail: andrew.kellett@dcu.ie


Dr. Z. Molphy, Prof. A. Kellett
 Synthesis and Solid-State Pharmaceutical Centre
 School of Chemical Sciences, Dublin City University
 Glasnevin, Dublin 9 (Ireland)

Prof. N. P. Farrell
 Department of Chemistry, Virginia Commonwealth University
 Richmond, VA 23284-2006 (USA)

Dr. D. Singleton, Prof. T. Brown
 ATDBio Ltd., School of Chemistry
 University of Southampton, Southampton, SO17 1BJ (UK)

Prof. T. Brown
 Chemistry Research Laboratory, University of Oxford
 12 Mansfield Road, Oxford OX1 3TA (UK)

 Supporting information and the ORCID identification number for one of the authors of this article can be found under: <https://doi.org/10.1002/anie.202110455>.

 © 2021 The Authors. Angewandte Chemie International Edition published by Wiley-VCH GmbH. This is an open access article under the terms of the Creative Commons Attribution Non-Commercial License, which permits use, distribution and reproduction in any medium, provided the original work is properly cited and is not used for commercial purposes.

platinum(II) complexes is not optimal for coordinating a DNA base within a TFO probe strand and crosslinking to a specific duplex target; 3) the rigid design of *trans*-Pt-TFOs means that hybrids have a very narrow target window dependent on the precise purine base location in the target strand; 4) post-synthetic procedures involving tethered chelators can alleviate rigidity problems but they are not compatible with ONs that contain purine nucleobases; and 5) solid-phase synthetic methods have, to date, been unsuccessful in generating functional Pt^{II}-TFOs.

Here, we present a new strategy for the generation of *cis*-platinum(II)-TFO hybrids that possess dsDNA binding and crosslinking activity. Pt^{II}-TFO hybrids were generated by conjugating an azide-modified *cis*-platinum(II) chemotype with an alkyne-modified TFO using both copper-catalysed azide-alkyne cycloaddition (CuAAC) and strain-promoted azide-alkyne cycloaddition (SPAAC) methods (Figure 1). Our group recently demonstrated how nucleic acid click chemistry can be applied to generate hybrid TFO molecular scissors that afford reliable targeted oxidative cleavage.^[15] Separately, elegant studies by DeRose and co-workers

demonstrated how azide-functionalised Pt^{II} complexes undergo click conjugation with alkyne fluorophores to enable identification of DNA crosslinking activity and cellular localisation properties.^[16] In the current study, azide groups were incorporated into *cis*-platinum(II) scaffolds to afford suitable handles for coupling with alkyne-modified TFOs through click chemistry. To maximise their crosslinking potential, platinum(II) complexes were designed to be geometrically and structurally similar to the clinical agents cisplatin, carboplatin, and oxaliplatin. We targeted purine-rich tracts of the green fluorescent protein (GFP) gene and assessed the Pt-TFO hybrid stability and crosslinking through thermal melting studies and native and denaturing PAGE analysis. The use of intercalator thiazole orange (TO) was further employed to develop a higher order class of Pt^{II}-TO-TFO hybrid oligonucleotide probes.

Results and Discussion

Azide-modified platinum(II) complexes possessing click chemistry potential while maintaining the traditional *cis*-platinum(II) structural properties were developed. Pt^{II} complexes *cis*-[Pt(2-azidopropane-1,3-diamine)Cl₂] (**5**, Pt-N₃-Cis), *cis*-[Pt(2-azidopropane-1,3-diamine)(CBDCA)] (**7**, Pt-N₃-Carbo, CBDCA = cyclobutane-1,1-dicarboxylate), and *cis*-[Pt(2-azidopropane-1,3-diamine)(Oxalate)] (**8**, Pt-N₃-Oxali) were generated according to Figure 2. 2-Azidopropane-1,3-diamine hydrochloride (**4**) was selected as a suitable bidentate ligand scaffold as it had been previously shown to be an efficient chelator for platinum while maintaining excellent click orthogonality.^[16a] Although **5** and **7** have previously been reported in the development of diazenecarboxamide-extended conjugates^[17]—**5** in the identification of platinum cellular protein targets^[18] and **7** further afield in mitochondrial localisation^[19] and clicked estrogen-hybrid generation^[20]—we here extend this concept to the oxaliplatin-like derivative **8**, which, to our knowledge, has not yet been reported. Additionally, no work has yet been performed to construct gene-targeting hybrids involving azide-Pt^{II} and alkyne-modified TFOs. All three target complexes were accessed through a common ligand, di-*tert*-boc-2-hydroxy-1,3-diaminopropane,

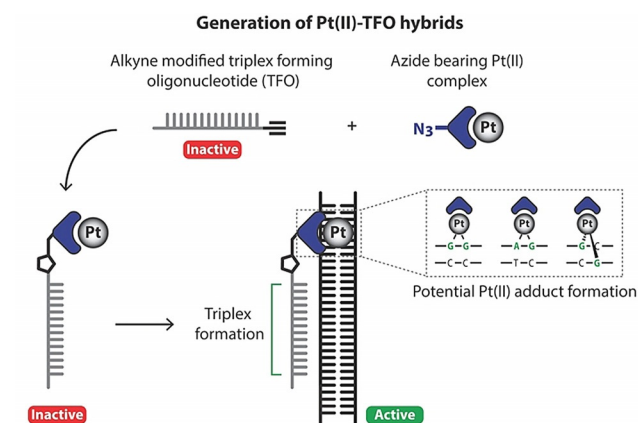


Figure 1. Overview of Pt^{II}-TFO hybrid design and application. Development of an azide-bearing platinum(II) complex prior to the generation of Pt^{II}-TFO hybrids by click chemistry. Triplex formation is obtained through parallel Hoogsteen binding to the target dsDNA. Crosslink formation with the duplex target is facilitated by the triplex formation.

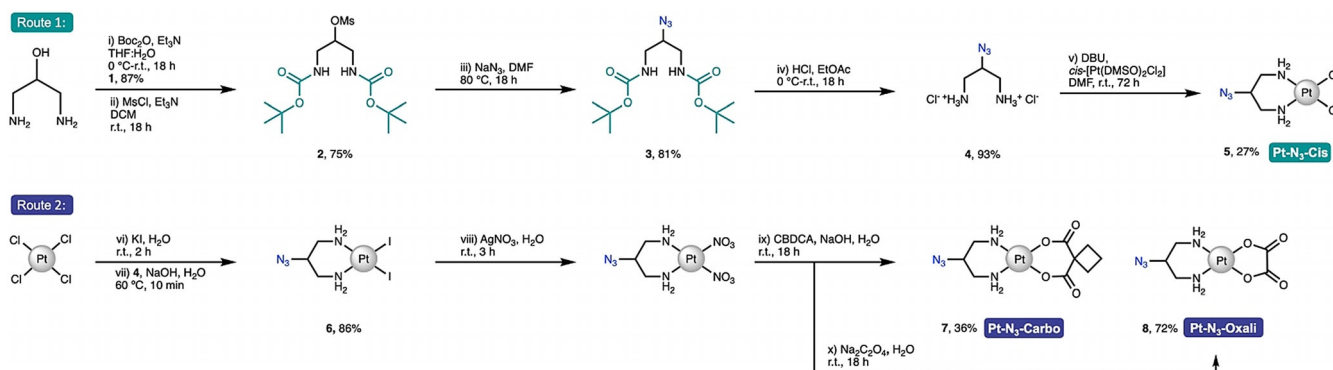


Figure 2. Synthetic routes for the preparation of azide-functionalised platinum(II) complexes. Route 1: Preparation of *cis*-[Pt(2-azidopropane-1,3-diamine)Cl₂] (Pt-N₃-Cis, **5**, 27%). Route 2: Preparation of *cis*-[Pt(2-azidopropane-1,3-diamine)(CBDCA)] (Pt-N₃-Carbo, **7**, 36%) and *cis*-[Pt(2-azidopropane-1,3-diamine)(Oxalate)] (Pt-N₃-Oxali, **8**, 72%).

which was obtained in excellent yields (**4**, 93 %) and allowed facile handling in subsequent reactions. Pt-N₃-Cis (**5**) was obtained through the treatment of **4** with *cis*-[PtCl₂(DMSO)₂] in the presence of DBU in the dark (Route 1, Figure 2). To obtain **7** and **8**, K₂PtI₄ (generated from K₂PtCl₄) was treated with **4** and substituted with either cyclobutane-1,1-dicarboxylic acid (CBDCA) or sodium oxalate to afford Pt-N₃-Carbo (**7**) or Pt-N₃-Oxali (**8**), respectively, in moderate (36 %) or high (72 %) yields (Route 2, Figure 2). The complexes were characterised by ¹H, ¹³C, and ¹⁹⁵Pt multinuclear NMR and FTIR spectroscopy as well as ESI-MS (see Figure S-2 for full details).

A range of ONs targeting a specific location of GFP plasmid DNA were selected. These TFOs were designed to incorporate alkyne-modified bases for functionalisation through click chemistry with azide-modified *cis*-platinum(II) complexes. The design of the TFOs included several considerations that have previously led to effective triplex formation, including: 1) TFOs were generated as homopyrimidine oligomers to afford effective Hoogsteen base recognition of the target duplex; 2) a low number of triplet inversions and mismatches were included to prevent destabilization; and 3) the number of consecutive C⁺-GC triplets was minimized to avoid electronic repulsion, which reduces their stabilising effects at low pH values. Pt^{II}-TFO hybrids were generated by clicking Pt-N₃-Cis (**5**), Pt-N₃-Carbo (**7**), or Pt-N₃-Oxali (**8**) to the alkyne-modified TFOs (Figure 3) as described in the Supporting Information (S-1.4). A library of five TFOs were developed that were between 21–29 nucleotides in length (Figure 3B). To investigate the effectiveness of platinum

crosslinking and triplex stability, terminal modified 5' (TFO1, 2, and 4), internal alkyne modifications (TFO3 and 5), base modifications of 5'-(5)octadiynyldeoxycytidine (TFO1 and 4), and internal-octadiynyldeoxyuridine (TFO3 and 5) and 5'-bicyclo[6.1.0]nonynedeoxycytidine (5'-BCN(CEP II)-dC) were employed (TFO2; Figure 3A). Triplexes formed by TFO1, 2, and 3 contained a single G-CG inversion, whereas TFO4 and 5 contained two G-CG inversion sites. Three target duplexes were synthesised that corresponded to the recognition elements of the GFP gene with an eight-nucleobase overhang introduced on the 5' side and a three-nucleotide overhang on the 3' side of the target purine sequence. These overhangs were designed to facilitate possible crosslinking activity and harbor numerous GG and/or AG steps—the preferred purine tract for traditional formation of *cis*-platinum(II) adducts. TFOs containing either octadiynyl-dC (TFO1 and 4) or octadiynyl-dU (TFO3 and 5) were reacted through a click reaction using the CuAAC method, while TFO2, containing the 5'-BCN(CEP-II)-dC, was generated following a SPAAC approach (see S-1.4). The complete library of Pt^{II}-TFO hybrids is provided in Table S-4.

Prior to triplex formation studies, thermal melting analysis was performed to investigate the binding interaction between the azide-functionalised *cis*-platinum(II) complexes and duplex target sequences from the GFP gene (Figure 4A). Melting experiments were performed under physiological conditions (10 mM phosphate, 150 mM NaCl, and 2 mM MgCl₂) following the procedure described in the Supporting Information (S-1.5). Native duplex melting temperatures were compared to those treated with the *cis*-platinum(II) complexes over 48 h (Figure 4B). All complexes destabilised

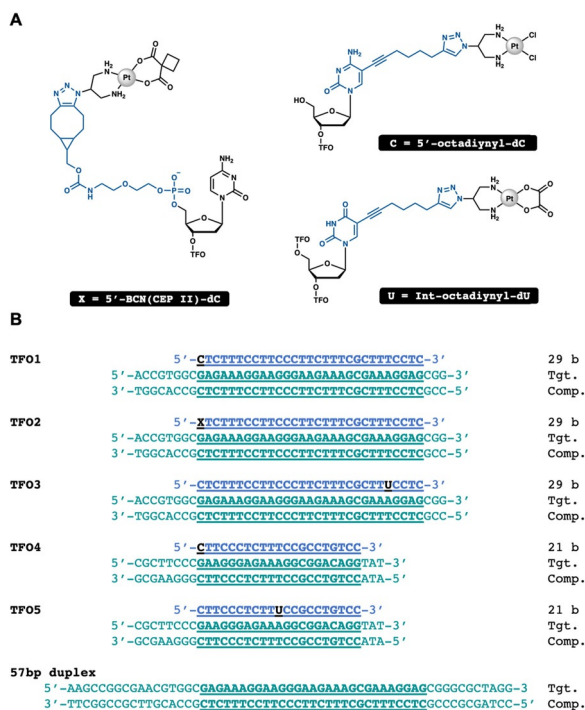


Figure 3. A) Alkyne-modified nucleobases. Click combination with each of the azide-functionalised platinum(II) complexes. B) TFO sequences with nucleobase modifications denoted and specific recognition sites indicated within the respective duplex target.

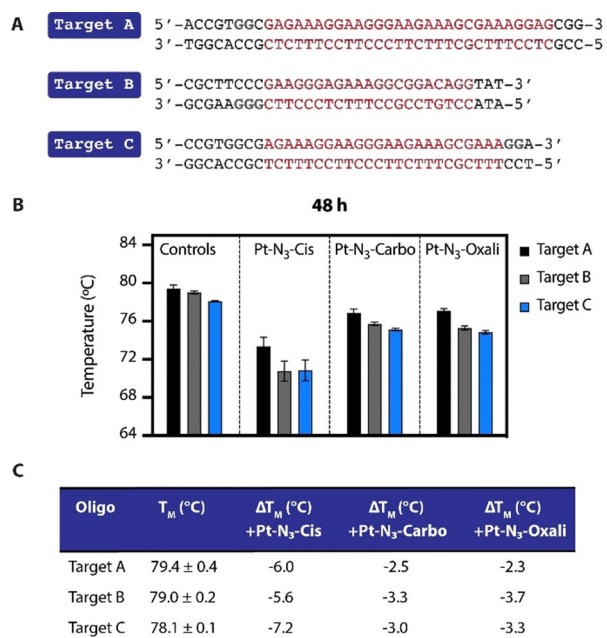


Figure 4. A) dsDNA sequences of the GFP gene, with the triplex recognition site shown in red. B) ΔT_M values of target dsDNA sequences treated with 2.5 equiv azide-functionalised platinum(II) complexes. C) Specific T_M values for duplex sequences when treated with Pt-N₃-Cis, Pt-N₃-Carbo, or Pt-N₃-Oxali.

the melting transition of the target duplexes to varying extents. Pt-N₃-Cis was found to have the greatest destabilising effect with decreases of 5.6–7.2 °C observed. Pt-N₃-Oxali and Pt-N₃-Carbo also reduced the melting temperatures of the three targets, but had notably lower destabilising effects than Pt-N₃-Cis. The observed thermal destabilisation effects can be ascribed to the binding of the *cis*-platinum(II) agents followed by kinking or conformational disruption of the duplex. Similarly, the greater activity of Pt-N₃-Cis relative to both Pt-N₃-Carbo and Pt-N₃-Oxali is in line with observations of the crosslinking effects of these clinical agents (S-7).^[21]

Triplex formation was investigated using UV thermal melting with analysis at pH 6 (S-1.5). All alkyne- and Pt^{II}-TFOs were purified prior to experimentation (S-1.2). Alkyne- and Pt^{II}-TFOs were incubated with duplex targets for 24 and 48 h in triplex buffer prior to T_M analysis. Triplex melting profiles were recorded for the alkyne-modified TFOs except for TFO4—a 21 nt terminal octadiynyl-dC—which melted below 12 °C. No differences were found in the melting profiles of the alkyne-TFOs over 24 and 48 h incubation periods. Melting analysis of the Pt^{II}-TFO hybrids showed pronounced results after 48 h of continuous incubation. Firstly, not all Pt^{II} hybrids were capable of triplex formation, including TFO1-Cis, TFO2-Cis, TFO4-Cis, and TFO5-Cis, which indicates that the cisplatin-type moiety, in the majority of cases, precludes triplex formation. TFO3-Cis was identified to form a DNA triplex after 24 h and the melting temperature was significantly lower than that of the control alkyne-TFO3. By 48 h, the melting temperature was more pronounced, with TFO3-Cis melting at 42.6 °C in comparison to 52.0 °C for the alkyne-TFO3 ($\Delta T_M = -9.4$ °C; Figure 5A). Unlike the TFO-Cis family, the Pt-N₃-Carbo and Pt-N₃-Oxali hybrids did not inhibit triplex formation, but their melting temperatures were reduced compared to the alkyne-TFO controls (S-6). Here, destabilisation was less pronounced than the triplex-forming N₃-Cis hybrids, although it was still substantial compared to the respective controls. Overall, the destabilisation induced by Pt^{II}-TFO hybrids alludes to potential crosslinking interactions between the platinum(II) ion and the target duplex, since destabilisation was identified as a key feature of platinum(II) crosslinking in earlier experiments (Figure 5B). To overcome stability limitations associated with Pt^{II}-TFOs, TO-modified constructs were developed with carboplatin-

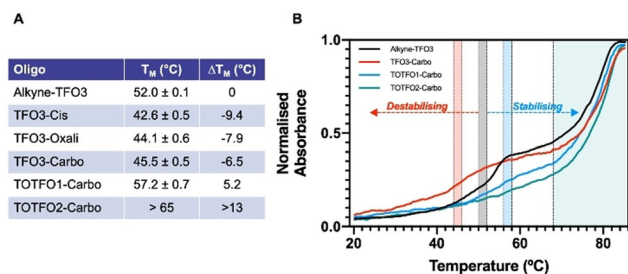


Figure 5. A) T_M values of triplex melting observed for TFO3 and TOTFO hybrids. B) Thermal melting curves showing destabilising and stabilising effects in comparison to alkyne-modified TFO3. Key: red = TFO3-Carbo; black = Alkyne-TFO3; blue = TOTFO1-Carbo; and cyan = TOTFO2-Carbo represent the respective mid-points of the triplex transitions.

type derivatives. TO-TFOs have previously demonstrated an ability to significantly enhance triplex stability^[22] through intercalation within the major groove of duplex targets—particularly the TO_{B6} modification (Figure S-25). Here, TFO hybrids were designed to incorporate both a carboplatin moiety and TO_{B6} modifications. Prior to click conjugation with N₃-Pt-Carbo, TO_{B6} was coupled to propargylamino-dU (pdU) nucleobases, as increased base stacking from the pdU triple bond has been shown to further improve triplex stabilisation.^[23] TOTFO1-Carbo, containing a single TO modification, displayed increased triplex stability ($\Delta T_M = +5.2$ °C) compared to alkyne-TFO3 (Figure 5A). Significantly, triplex stability increased by +11.7 °C compared to TFO3-Carbo, thus demonstrating that the formation of the Pt^{II}-TFO triplex can be stabilised by the addition of a single TO unit. TOTFO2-Carbo, which incorporates two TO_{B6} units, was then shown to push triplex melting to a similar temperature as the underlying duplex transition (Figure 5B), with PAGE analysis confirming combined triplex formation and fluorescence emission by the TO_{B6} units (Figure S-25).

Since hybrids of TFO3 displayed the greatest thermal destabilisation upon triplex formation, these constructs were investigated for their crosslinking activity. Triplex formation was performed in the presence of a 57 bp target duplex and an off-target 40 bp duplex sequence (Figure 6A). The off-target sequence retains numerous GG and AG base steps to encourage adduct formation; however, it does not possess

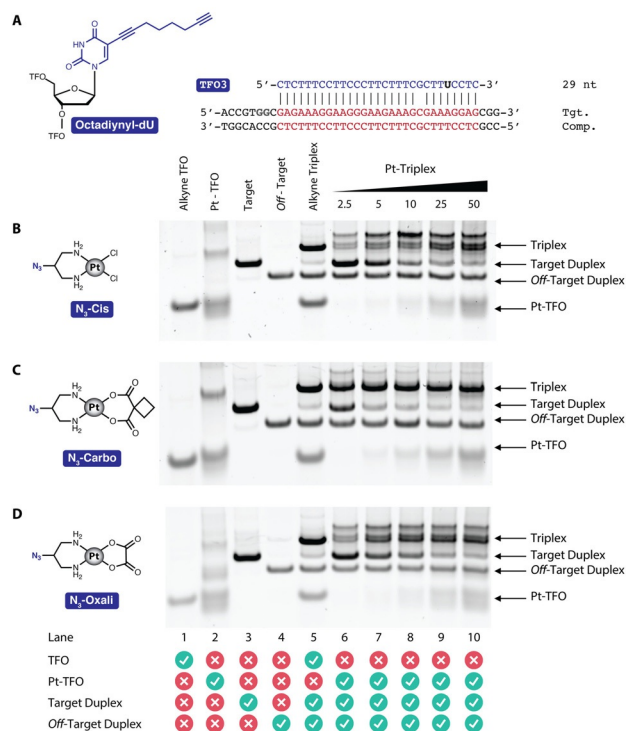


Figure 6. A) TFO3 with modified internal octadiynyl-dU nucleobase and respective GFP target sequence. B) TFO3-Cis hybrid triplex formation with higher band structures observable. C) TFO3-Carbo hybrid. Triplex formation is significant even at lower loadings. D) TFO3-Oxali hybrid with higher band triplex formation—slower rate of triplex formation in comparison with TFO3-Carbo.

the triplex recognition site. Target and off-target sequences were mixed in triplex buffer in a 1:1 ratio (1 pmol) prior to the introduction of increasing concentrations of the hybrid (2.5–50 equiv; Figure 6B–D, lanes 6–10) and incubated at 37°C for 48 h. Evidence of concentration-dependent triplex formation can be seen in all three of the sample-treated experiments while, notably, no diminishment of the off-target duplex was observed. The ablation of target duplex can be seen as triplex formation increases, and this reduction coincides with the respective thermal destabilising capabilities of the hybrid moieties, whereby TFO3-Carbo triplex formation occurs at the lowest loading (Figure 6C), followed thereafter by TFO3-Oxali and TFO3-Cis. Significantly, TFO3-Cis and TFO3-Oxali (Figure 6B,D) displayed higher order triplex banding patterns compared to the alkyne-TFO (lane 5), which indicates a variety of crosslinked triplexes have formed. Taken together, it is likely that the most active hybrid, TFO3-Carbo, forms one predominant crosslink with the target duplex, while the Cis and Oxali derivatives form a variety of adducts.

As a consequence of the greater *trans* substitution effect of the cyanido (CN⁻) ligand compared to am(m)ine, the cyanido ligand is known to be a strong substituting group for platinum(II) and thus is capable of removing a Pt^{II} adduct from the N7-position of guanine nucleobases.^[24] Treatment of crosslinked DNA with a NaCN solution results in the formation of the highly stable [Pt(CN)₄]²⁻ complex and a return to the native state for the target duplex sequence. Prior to verifying crosslinking between the Pt^{II}-TFO hybrids and the duplex target, alkyne-TFO3 (50 pmol) was incubated with target duplex 3 (D3; 1 pmol; Figure 7A) for 48 h prior to the addition of up to 25000 equiv of NaCN to identify its effect on triplex formation (Figure 7B). The probe used in this study (D3) is a 40 bp target sequence that contains the TFO recognition site, with a Cy5 fluorescent tag located at the 5'-terminus of the purine strand and a 6-FAM fluorescent tag adjoined to the 5'-terminus of the complementary pyrimidine strand. At the higher loading of NaCN (>10000 equiv), triplex stability was demonstrably affected

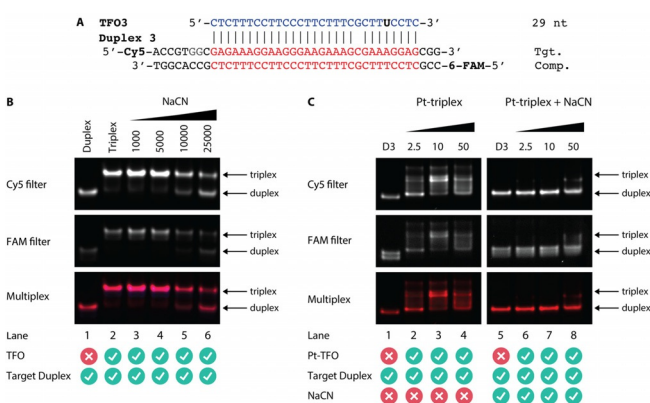


Figure 7. A) TFO3-Cis hybrid and fluorescently labelled duplex 3. B) NaCN treatment of the unmodified triplex system. C) NaCN (5000 equiv) afforded reversal of the Pt-triplex system formed by the TFO3-Cis hybrid. Figure 7B (Cy5) was taken from a section of Figure S-26.

with progressive triplex depletion and reformation of the duplex notable (Figure 7B, lanes 3–6). Treating D3 with TFO3-Cis (2.5–50 equiv) in the absence of NaCN revealed crosslinking activity, with a banding pattern indicative of multiple higher-order triplex structures (Figure 7C, lanes 2–4). Upon treatment with NaCN (5000 equiv) complete reversal of the TFO-Cis crosslinking and triplex formation was observed (Figure 7C, lanes 6–8). Comparison of this result with that of the unmodified alkyne-TFO3 control under identical conditions (Figure 7B, lane 4) provides strong evidence of crosslinking activity by the hybrid.

Since triplex-mediated crosslinking activity has been established, further analysis of the sequence-specific binding was examined using denaturing PAGE experiments outlined in Figure 8A. Here, 17-mer alkyne-TFO sequences were designed and clicked to the Pt-N₃-Carbo complex (Figure 8B). TFOs were designed to incorporate 5', 3', and internal alkyne base modifications (Figure 8C, S-4). A duplex target consisting of a 21 nt purine sequence with a Cy-5 fluorescent label at the 5'-terminus and a 17 nt pyrimidine complementary strand labelled with a 6-FAM fluorophore was employed. Similarly, a duplex target consisting of complementary 21-mer strands was employed; however, denaturing of this duplex sequence proved to be ineffective. The target duplexes (21:17D and 21:21D; 1 pmol) were treated with 50 equiv of each hybrid and incubated for at least 48 h at 37°C. Denaturing PAGE identified crosslinking with only the purine strand of the target duplex, as verified by the Cy-5 filter emission for terminally modified TFO-17A-Carbo and TFO-17B-Carbo (Figure 8D). TFO-17C Carbo did not display any crosslinking activity and this may be due to the

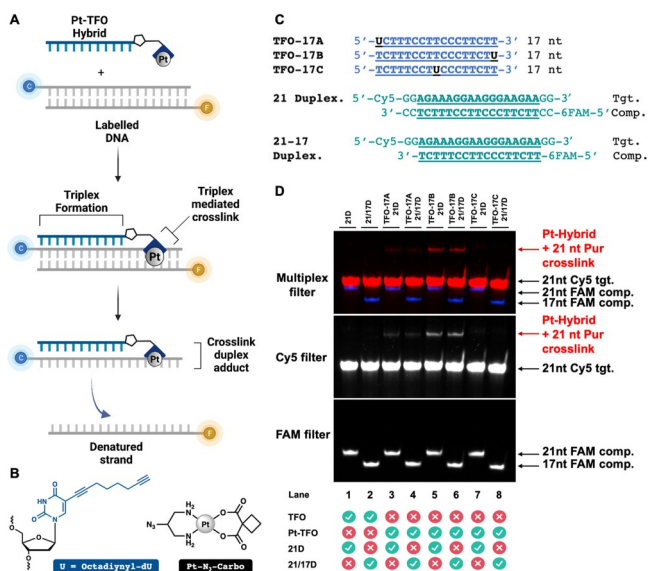


Figure 8. A) Design of the denaturing PAGE experiment. B) Terminal and internal nucleobase modification of octadiynyl-dU and azide-functionalised Pt-N₃-Carbo. C) Modified TFO sequences and dsDNA targets. D) Denaturing PAGE analysis: TFO-hybrids (50 equiv) were incubated at 37°C with duplex targets in triplex buffer for a minimum of 48 h prior to electrophoresis. The upper band (lanes 3–6) observed under a Cy5 filter is indicative of adduct formation with the purine strand. No adduct formation observed for TFO-17C (lanes 7 and 8).

centrally located alkyne modification site. Thus, in the case of shorter Pt^{II}-TFO hybrids, it appears that terminal modifications are required for appropriate crosslinking activity. A general summary regarding CuAAC and SPAAC^[25] click chemistry strategies employed here can be found in the Supporting Information (S-10 and Table S-5).

Conclusion

This study has demonstrated the development and application of a potential new class of platinum(II)-TFO hybrids. To our knowledge, the use of nucleic acid click chemistry to combine a TFO vector with azide-functionalised *cis*-platinum(II) complexes represents the first examples of platinum(II)-TFO hybrids designed in this way. In comparison to existing methods used to prepare platinated TFOs, click chemistry affords a modular approach whereby the incorporation of *cis*-platinum(II) at practically any location within the probe strand is possible. This approach also overcomes limitations that require complexation between a platinum(II) reagent, such as a *trans*-platinum(II) complex,^[10a,b] and the TFO substrate—an approach that hitherto precluded the development of *cis*-platinum(II)-type hybrids^[14a] and the ability to generate 1,2-d(GpG) cisplatin lesions central to their clinical success. The use of PAGE analysis indicates that, for several TFO constructs, numerous platinated triplex adducts can form, giving rise to distinctive banding patterns that are reversed upon removal of the crosslink with sodium cyanide. Finally, targeting of the purine:pyrimidine strand by platinum(II)-TFO hybrids was investigated by denaturing fluorescently labelled duplex sequences, with crosslinking evident within the purine strand only. Overall, this study demonstrates a modular approach to the development of *cis*-platinum(II)-TFO hybrids with recognition and targeting of specific genetic elements possible through triplex-mediated binding. Stability limitations are inherent to triplex motifs and, in these constructs, care must be taken to avoid further destabilisation through the choice and positioning of the *cis*-platinum(II) unit. Crucially, the inclusion of TO intercalators appears to augment triplex stability and prevents the destabilisation effects imposed by the linked platinum(II) complex. A future approach to fully realise the biological potential of these *cis*-platinum(II) hybrids within antigene technology may involve the use of modifications such as phosphorothioate backbone linkages, phosphorodiamidate morpholino oligonucleotides, and ribose modifications. These modifications must be combined with a unique targeting strategy, whereby mutant genes or oncogenes—particularly those present in recalcitrant cancers such as triple-negative breast cancer or glioblastoma multiforme—are specifically targeted by this technology to achieve selectivity over normal cells.

Acknowledgements

A.K. acknowledges funding from the Science Foundation Ireland Career Development Award (SFI-CDA) [15/CDA/

3648]. J.H. and B.McG acknowledge funding from the Irish Research Council and [GOIPG/2016/1117] and [GOIPG/2018/1427], respectively. This publication has emanated from research supported in part by a research grant from the Science Foundation Ireland (SFI) and is co-funded under the European Regional Development Fund under Grant Number 12/RC/2275 P2. UV and fluorescence spectroscopy were carried out at the Nano Research Facility at Dublin City University, which was funded under the Programme for Research in Third Level Institutions (PRTL) Cycle 5. The PRTL is co-funded through the European Regional Development Fund (ERDF), part of the European Union Structural Funds Programme 2011–2015. Figure 8A was created with BioRender. Open access funding provided by IReL.

Conflict of Interest

The authors declare no conflict of interest.

Keywords: click chemistry · crosslinking · DNA hybrids · DNA triplex · platinum

- [1] a) X. Shen, D. R. Corey, *Nucleic Acids Res.* **2018**, *46*, 1584–1600; b) S. T. Crooke, B. F. Baker, R. M. Crooke, X.-H. Liang, *Nat. Rev. Drug Discovery* **2021**, *20*, 427–453.
- [2] K. R. Fox, *Curr. Med. Chem.* **2000**, *7*, 17–37.
- [3] K. R. Fox, T. Brown, D. A. Rusling, in *DNA-Targeting Molecules as Therapeutic Agents* (Ed.: M. J. Waring), Royal Society of Chemistry, Cambridge, **2018**, pp. 1–32.
- [4] a) J.-S. Sun, T. Carestier, C. Hélène, *Curr. Opin. Struct. Biol.* **1996**, *6*, 327–333; b) P. E. Nielsen, *Annu. Rev. Biophys. Biomol. Struct.* **1995**, *24*, 167–183.
- [5] a) M. Takasugi, A. Guendouz, M. Chassignol, J. L. Decout, J. Lhomme, N. T. Thuong, C. Helene, *Proc. Natl. Acad. Sci. USA* **1991**, *88*, 5602–5606; b) P. A. Havre, E. J. Gunther, F. P. Gasparro, P. M. Glazer, *Proc. Natl. Acad. Sci. USA* **1993**, *90*, 7879–7883.
- [6] D. Oh, *Nucleic Acids Res.* **1999**, *27*, 4734–4742.
- [7] M. Kundu, F. Nagatsugi, A. Majumdar, P. S. Miller, M. M. Seidman, *Nucleosides Nucleotides Nucleic Acids* **2003**, *22*, 1927–1938.
- [8] R. Besch, C. Giovannangeli, T. Schuh, C. Kammerbauer, K. Degitz, *J. Mol. Biol.* **2004**, *341*, 979–989.
- [9] a) I. Dieter-Wurm, M. Sabat, B. Lippert, *J. Am. Chem. Soc.* **1992**, *114*, 357–359; b) C. Colombier, B. Lippert, M. Leng, *Nucleic Acids Res.* **1996**, *24*, 4519–4524; c) E. Bernal-Méndez, J.-S. Sun, F. González-Vílchez, M. Leng, *New J. Chem.* **1998**, *22*, 1479–1483; d) E. S. Gruff, L. E. Orgel, *Nucleic Acids Res.* **1991**, *19*, 6849–6854.
- [10] a) M. A. Campbell, T. M. Mason, P. S. Miller, *Can. J. Chem.* **2007**, *85*, 241–248; b) M. A. Campbell, P. S. Miller, *J. Biol. Inorg. Chem.* **2009**, *14*, 873–881; c) M. A. Campbell, P. S. Miller, *Bioconjugate Chem.* **2009**, *20*, 2222–2230; d) M. K. Graham, P. S. Miller, *J. Biol. Inorg. Chem.* **2012**, *17*, 1197–1208; e) M. K. Graham, T. R. Brown, P. S. Miller, *Biochemistry* **2015**, *54*, 2270–2282.
- [11] R. Manchanda, S. U. Dunham, S. J. Lippard, *J. Am. Chem. Soc.* **1996**, *118*, 5144–5145.
- [12] K. S. Schmidt, D. V. Filippov, N. J. Meeuwenoord, G. A. van der Marel, J. H. van Boom, B. Lippert, J. Reedijk, *Angew. Chem. Int. Ed.* **2000**, *39*, 375–377; *Angew. Chem.* **2000**, *112*, 383–385.

- [13] D. Cech, J. Schliepe, U. Berghoff, B. Lippert, *Angew. Chem. Int. Ed. Engl.* **1996**, *35*, 646–648; *Angew. Chem.* **1996**, *108*, 705–707.
- [14] a) S. K. Sharma, L. W. McLaughlin, *J. Am. Chem. Soc.* **2002**, *124*, 9658–9659; b) S. K. Sharma, L. W. McLaughlin, *J. Inorg. Biochem.* **2004**, *98*, 1570–1577.
- [15] a) T. Lauria, C. Slator, V. McKee, M. Müller, S. Stazzoni, A. L. Crisp, T. Carell, A. Kellett, *Chem. Eur. J.* **2020**, *26*, 16782–16792; b) N. Zuin Fantoni, B. McGorman, Z. Molphy, D. Singleton, S. Walsh, A. H. El-Sagheer, V. McKee, T. Brown, A. Kellett, *ChemBioChem* **2020**, *21*, 3563–3574.
- [16] a) A. D. Moghaddam, J. D. White, R. M. Cunningham, A. N. Loes, M. M. Haley, V. J. DeRose, *Dalton Trans.* **2015**, *44*, 3536–3539; b) R. Wirth, J. D. White, A. D. Moghaddam, A. L. Ginzburg, L. N. Zakharov, M. M. Haley, V. J. DeRose, *J. Am. Chem. Soc.* **2015**, *137*, 15169–15175.
- [17] a) D. Urankar, J. Košmrlj, *Inorg. Chim. Acta* **2010**, *363*, 3817–3822; b) N. Stojanović, D. Urankar, A. Brozović, A. Ambriović-Ristov, M. Osmak, J. Košmrlj, *Acta. Chim. Slov.* **2013**, *60*, 368–374.
- [18] R. M. Cunningham, V. J. DeRose, *ACS Chem. Biol.* **2017**, *12*, 2737–2745.
- [19] V. Reshetnikov, S. Daum, C. Janko, W. Karawacka, R. Tietze, C. Alexiou, S. Paryzhak, T. Dumych, R. Bilyy, P. Tripal, B. Schmid, R. Palmisano, A. Mokhir, *Angew. Chem. Int. Ed.* **2018**, *57*, 11943–11946; *Angew. Chem.* **2018**, *130*, 12119–12122.
- [20] E. Kitteringham, E. Andriollo, V. Gandin, D. Montagner, D. M. Griffith, *Inorg. Chim. Acta* **2019**, *495*, 118944.
- [21] L. Kelland, *Nat. Rev. Cancer* **2007**, *7*, 573–584.
- [22] S. Walsh, A. H. El-Sagheer, T. Brown, *Chem. Sci.* **2018**, *9*, 7681–7687.
- [23] J. Bijapur, S. Bergqvist, T. Brown, M. D. Keppler, K. R. Fox, *Nucleic Acids Res.* **1999**, *27*, 1802–1809.
- [24] S. J. Lippard, J. D. Hoeschele, *Proc. Natl. Acad. Sci. USA* **1979**, *76*, 6091–6095.
- [25] E. M. Sletten, C. R. Bertozzi, *Angew. Chem. Int. Ed.* **2009**, *48*, 6974–6998; *Angew. Chem.* **2009**, *121*, 7108–7133.

Manuscript received: August 4, 2021

Revised manuscript received: October 11, 2021

Accepted manuscript online: October 15, 2021

Version of record online: December 3, 2021